

Meteorology and Ozone, Temperature, Relative Humidity

J. Coates¹ and T. Butler¹

¹Institute for Advanced Sustainability Studies, Potsdam, Germany

October 29, 2015

Abstract

1 Introduction

Gap: Many observational studies have noted the dependence of ozone production on temperature and also the non-linearity of ozone production on temperature and NO_x. Furthermore, many regional modelling studies have also reproduced this relationship of ozone production on temperature for specific areas; currently most of these modelling studies have been concerned with US regions. Despite all this research, there has not been (to our knowledge) a detailed process study looking at modelled ozone as a function of both NO_x and temperature. In this study, we model ozone over various temperature and NO_x levels to determine how ozone production varies under these range of conditions. The review of Pusede et al. (2015) also highlights a lack of modelling studies looking at this non-linear relationship of ozone on NO_x and temperature.

Pusede et al. (2014) demonstrated the importance of tackling high ozone levels also from the stand point of temperature and in relation to varying NO_x conditions over the San Joaquin Valley in California and the review of Pusede et al. (2015) highlights that the temperature dependence of biogenic VOC (BVOC) emissions is mainly responsible for this relationship. In this study, we model the effects of temperature-dependent and temperature-independent BVOC emissions on ozone production in order to look at the effects of temperature dependent ozone production chemistry without temperature dependent VOC emissions and then the effects of temperature-dependent chemistry and temperature-dependent BVOC emissions. As mentioned

in the review of Pusede et al. (2015), typically BVOC emissions are temperature-dependent while anthropogenic VOC (AVOC) emissions tend to be temperature-independent, as AVOC emissions tend to be process and combustion related.

2 Methodology

2.1 Model Setup

- MECCA box model as described in Coates and Butler (2015) to broadly simulate the Benelux (Belgium, Netherlands and Luxembourg) region. As photolysis rates are parameterised by the solar zenith angle, the solar zenith angle of 51°N was used, representative of the central Benelux region.
- MECCA box model has been updated to include vertical mixing with the free troposphere and accordingly includes a diurnal cycle for the PBL height. These amendments are discussed further in Sect. 2.4.
- Simulations start at 06:00 using spring equinoctical conditions and the simulations ended after two days.
- All simulations performed using the Master Chemical Mechanism, MCM v3.2, (Rickard et al., 2015), Common Representative Intermediates, CRI v2 (Jenkin et al., 2008), Model for Ozone and related chemical tracers, MOZART-4 (Emmons et al., 2010), Regional Acid Deposition Model, RADM2 (Stockwell et al., 1990) and the Carbon Bond Mechanism, CB05 (Yarwood et al., 2005). Coates and Butler (2015) describes the implementation of these chemical mechanisms for use with KPP within MECCA. These chemical mechanisms were chosen as they are commonly used by modelling groups and represent the highly-detailed chemistry (MCM v3.2), chemistry suitable for regional 3D models (CRI v2, RADM2 and CB05) and global 3D models (MOZART-4).
- NO_x emissions and temperature were varied systematically to analyse the effects on ozone mixing ratios over different NO_x gradients and different temperatures.
- VOC emissions constant until noon of first day, to simulate a plume of emitted VOC.
- Two sets of runs were performed – to include both a temperature-dependent and temperature-independent source of biogenic VOC emissions. MEGANv2.1 (Guenther

et al., 2012) was used to specify the temperature-dependent BVOC emissions of isoprene. Isoprene is the most important VOC at a global scale due its high emission rates and emissions from vegetation have been reported to depend on temperature (Guenther et al., 2006).

- Methane is fixed at 1.7 ppmv throughout the model run, carbon monoxide (CO) and ozone were initialised at 200 ppbv and 40 ppbv and then allowed to evolve freely throughout the the simulation.
- The only source of NO_x emissions in the box model was a constant source of NO emissions. The NO emissions were systematically varied from 5.0×10^9 to 1.5×10^{12} molecules (NO) cm⁻² s⁻¹ at each temperature point used in this study. The temperature was systematically varied between 288 and 313 K (15 – 40 °C).

2.2 VOC Emissions

- Anthropogenic emissions from Benelux for the year 2011 were obtained from the TNO-MACC_III emission inventory. TNO-MACC_III is the current version of the TNO-MACC_II inventory and was created using the same methodology as Kuenen et al. (2014) and based upon improvements to the existing emission inventory during the AQMEII-2 exercises described in Pouliot et al. (2015).
- Temperature-independent emissions of the biogenic VOC isoprene and monoterpenes, were calculated as a fraction of the total anthropogenic VOC emissions from each country in the Benelux region, this data was obtained from the supplementary data available from the EMEP (European Monitoring and Evaluation Programme) model (Simpson et al., 2012).
- AVOC and BVOC emissions are included as total emissions from SNAP (Selected Nomenclature for Air Pollution) source categories and these emissions were assigned to chemical groupings based on the country specific profiles for Belgium, the Netherlands and Luxembourg provided by TNO.
- The MCM v3.2 initial species were determined using the country specific profiles for each SNAP source category and where appropriate information of individual chemical species that can be represented by MCM v3.2 were determined using the detailed speciations of

Table 1: Total anthropogenic NMVOC emissions in 2011 in tonnes from each SNAP category assigned from TNO-MACC_III emission inventory and biogenic VOC emission in tonnes from Benelux region assigned from EMEP. The allocation of these emissions to MCM v3.2, CRI v2, CB05, MOZART-4 and RADM2 species is found in the supplement.

	SNAP1	SNAP2	SNAP34	SNAP5	SNAP6	SNAP71
Belgium	4494	9034	22152	5448	42809	6592
Netherlands	9140	12173	29177	8723	53535	16589
Luxembourg	121	44	208	1371	4482	1740
Total	13755	21251	62648	15542	100826	24921
	SNAP72	SNAP73	SNAP74	SNAP8	SNAP9	BVOC
Belgium	2446	144	210	6448	821	7042
Netherlands	3230	1283	1793	10067	521	1462
Luxembourg	1051	6	324	643	0	2198
Total	6727	1433	2327	17158	1342	10702

Passant (2002). This approach was also used in von Schneidmesser et al. (2015) and further details are found within this article.

- As in von Schneidmesser et al. (2015), first the primary VOC that are represented by the MCM v3.2 and respective emissions were determined. Using this MCM v3.2 data, the NMVOC emission data were mapped to mechanism species in the other four chemical mechanisms used in the study. The NMVOC emissions in the non-MCM v3.2 chemical mechanisms were weighted by the carbon numbers of the MCM v3.2 species and the emitted mechanism species. The supplementary data outlines the primary NMVOC and calculated emissions with each chemical mechanism.

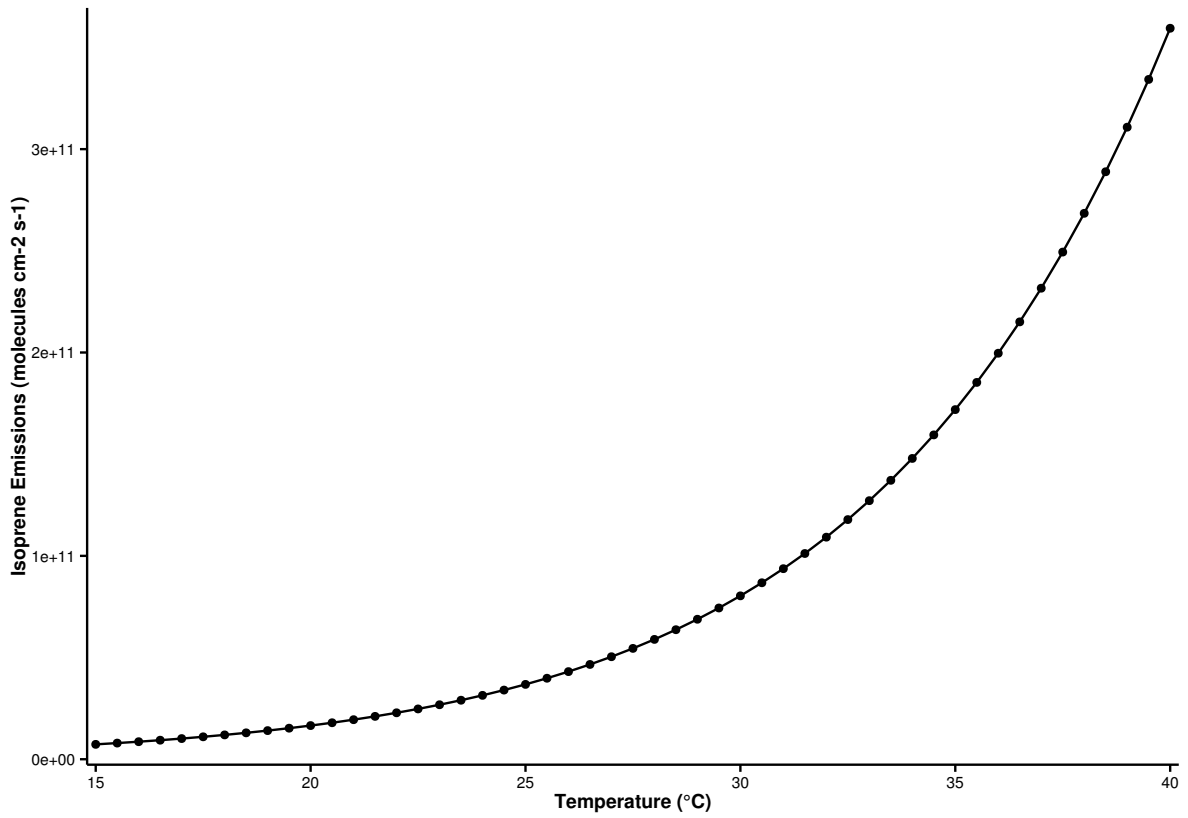
2.3 Temperature Dependent Isoprene Emissions

- Temperature dependent isoprene emissions were estimated using the MEGAN2.1 algorithm (Guenther et al., 2012).
- The aim of the study is to look at the effects of temperature, hence in the MEGAN2.1 algorithm all parameters (except temperature) were kept constant.
- The boxmodel setup uses a constant temperature throughout the model run and so the parameters T_{24} and T_{240} , the average temperatures in the past 24 and 250 hours, were assumed to be constant and equal to the temperature value of the boxmodel.
- Constant PAR (photosynthetically active radiation) and LAI (leaf area index) were used at each temperature step.
- The LAI, plant functional type (PFT) and associated isoprene emission factor were taken from Guenther et al. (2012) and selected to give the same isoprene mixing ratios at a temperature of 293 K as in the temperature independent modelling case. For all other model runs over the different temperature, the MEGAN2.1 algorithm was used to estimate the isoprene emissions.
- Thus using this idealised case, we can determine the effects of increasing isoprene emissions with temperature across NO_x gradients.
- This was repeated for each chemical mechanism.
- As in the temperature independent model runs, the emissions of NMVOC and the temperature dependent source of isoprene, were held constant until noon of the first day.
- Using these assumptions, the isoprene emissions at each temperature step of the study are illustrated in Fig. 1 and show the expected exponential increase in emissions with temperature (Guenther et al., 2006).

2.4 Vertical Mixing with Diurnal Boundary Layer Height

- The MECCA box model used in Coates and Butler (2015) included a constant boundary layer height of 1 km and no interactions (vertical mixing) with the free troposphere.

Figure 1: The estimated isoprene emissions (molecules isoprene $\text{cm}^{-2} \text{s}^{-1}$) at each temperature step used in the study. Isoprene emissions were estimated using the MEGAN2.1 algorithm (Guenther et al., 2012).



- The planetary boundary layer (PBL) height varies diurnally and affects chemistry by diluting emissions after sunrise when the PBL rises. The expansion of the PBL into the free troposphere introduces vertical mixing with those chemical species present in the free troposphere. When the PBL collapses in the evening, pollutants are trapped in the PBL.
- The mixing layer height was measured as part of the BAERLIN campaign over the city of Berlin. The profile of mean mixing layer height during the campaign period (June – August 2014) was used in the model to represent the diurnal cycle of the mixing layer height.
- The concentrations of the chemical species within the PBL are diluted due to the larger mixing volume when the PBL height increases at the beginning of the day, also the increasing PBL height mixes the chemical species from the free troposphere with the chemical species within the PBL i.e. vertical mixing. The PBL height collapses during night leaving the stable nocturnal boundary layer, trapping the chemical species into a smaller volume thus increasing the concentrations of the chemical species.
- This vertical mixing scheme was implemented into the boxmodel using the same approach of Lourens (2012).
- The mixing ratios of O₃, CO and CH₄ in the free troposphere were respectively set to 50 ppbv, 116 ppbv and 1.8 ppmv. These conditions were taken from the MATCH-MPIC chemical weather forecast model on the 21st March (the start date of the simulations). The model results (<http://cwf.iass-potsdam.de/>) at the 700 hPa height were chosen and the daily average was used as input into the boxmodel.

Reference
Boris'
paper

check
reference

3 Results

3.1 Ozone mixing ratios as function of NO_x and Temperature

Figure 2 depicts the maximum mixing ratio of ozone obtained from each model run as a function of the total NO_x emissions on the first day and temperature. Using each mechanism, a similar non-linear relationship of ozone mixing ratios on NO_x and temperature is found and increased ozone levels are found at higher temperatures when including a temperature-dependent source of isoprene emissions. CB05 and RADM2 produce the largest amount of ozone at higher temperatures than the other chemical mechanisms. A temperature-dependent source of isoprene, leads to more efficient ozone production as at higher temperature a lower amount of NO_x is

how?
prove
this

Figure 2: Contours of maximum ozone mixing ratio as a function of the total NO_x emissions on the first day and daily temperature for each chemical mechanism and using both a temperature-dependent and -independent source of isoprene emissions.

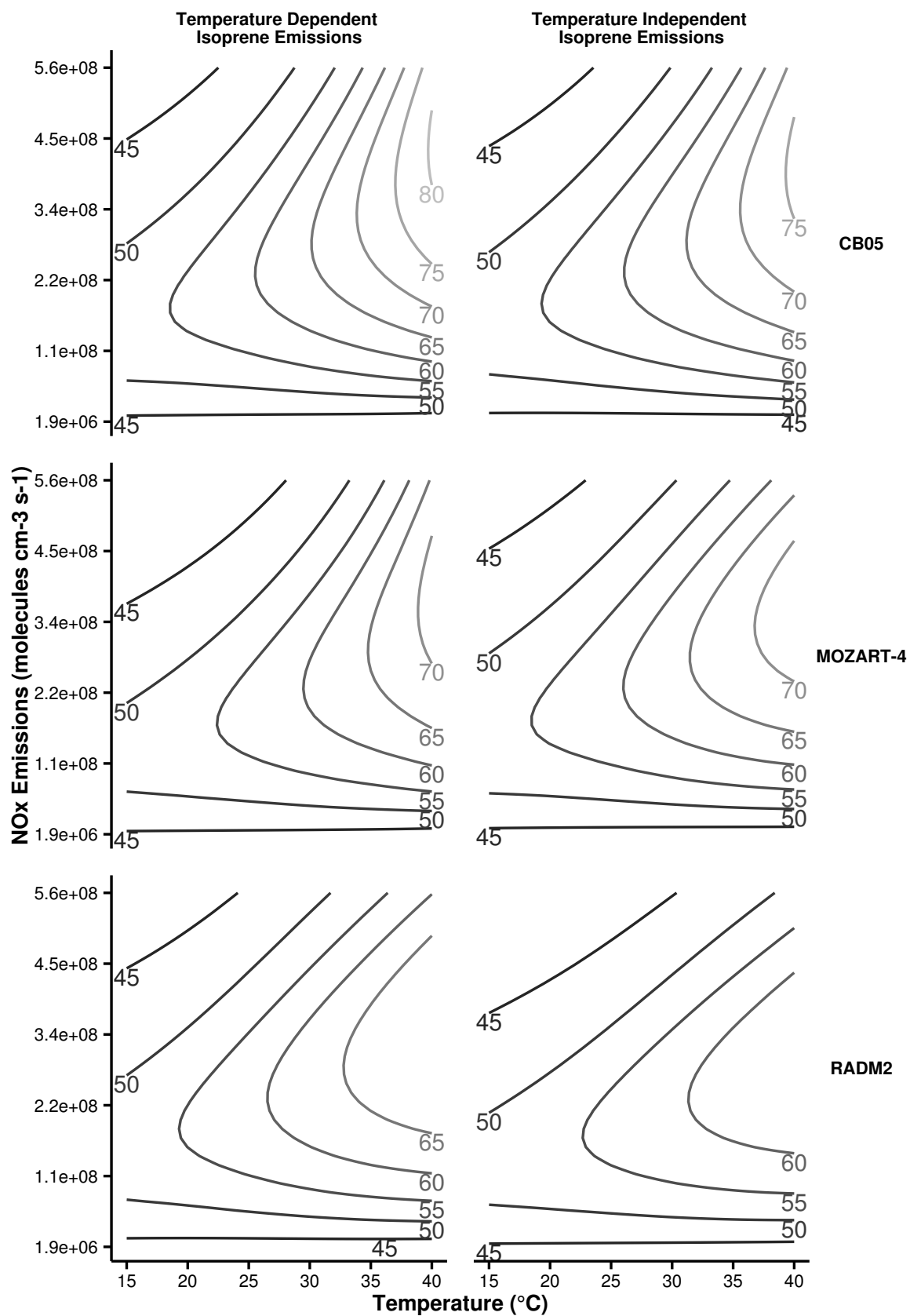


Table 2: Regression statistics for the linear relationship between ozone mixing ratios and temperature shown in Figure 3.

Mechanism	NO _x Condition	Temperature Dependent Isoprene Emissions		Temperature Independent Isoprene Emissions	
		Slope (m_{O_3-T})	R^2	Slope (m_{O_3-T})	R^2
CB05	Low-NO _x	0.96	0.96	0.72	0.99
	Maximal-O ₃	1.04	0.96	0.79	0.99
	High-NO _x	1.07	0.96	0.81	0.99
MOZART-4	Low-NO _x	0.70	0.97	0.48	1.00
	Maximal-O ₃	0.76	0.97	0.52	1.00
	High-NO _x	0.78	0.97	0.53	1.00
RADM2	Low-NO _x	0.84	0.98	0.66	1.00
	Maximal-O ₃	0.91	0.98	0.72	1.00
	High-NO _x	0.92	0.98	0.72	1.00

required to produce the same amount of ozone as when using a temperature-independent source of isoprene. At low temperature and high NO_x, similar amounts of ozone are predicted from both the temperature-dependent and temperature-independent sources of isoprene emissions.

3.2 Rate of Change of Ozone with Temperature

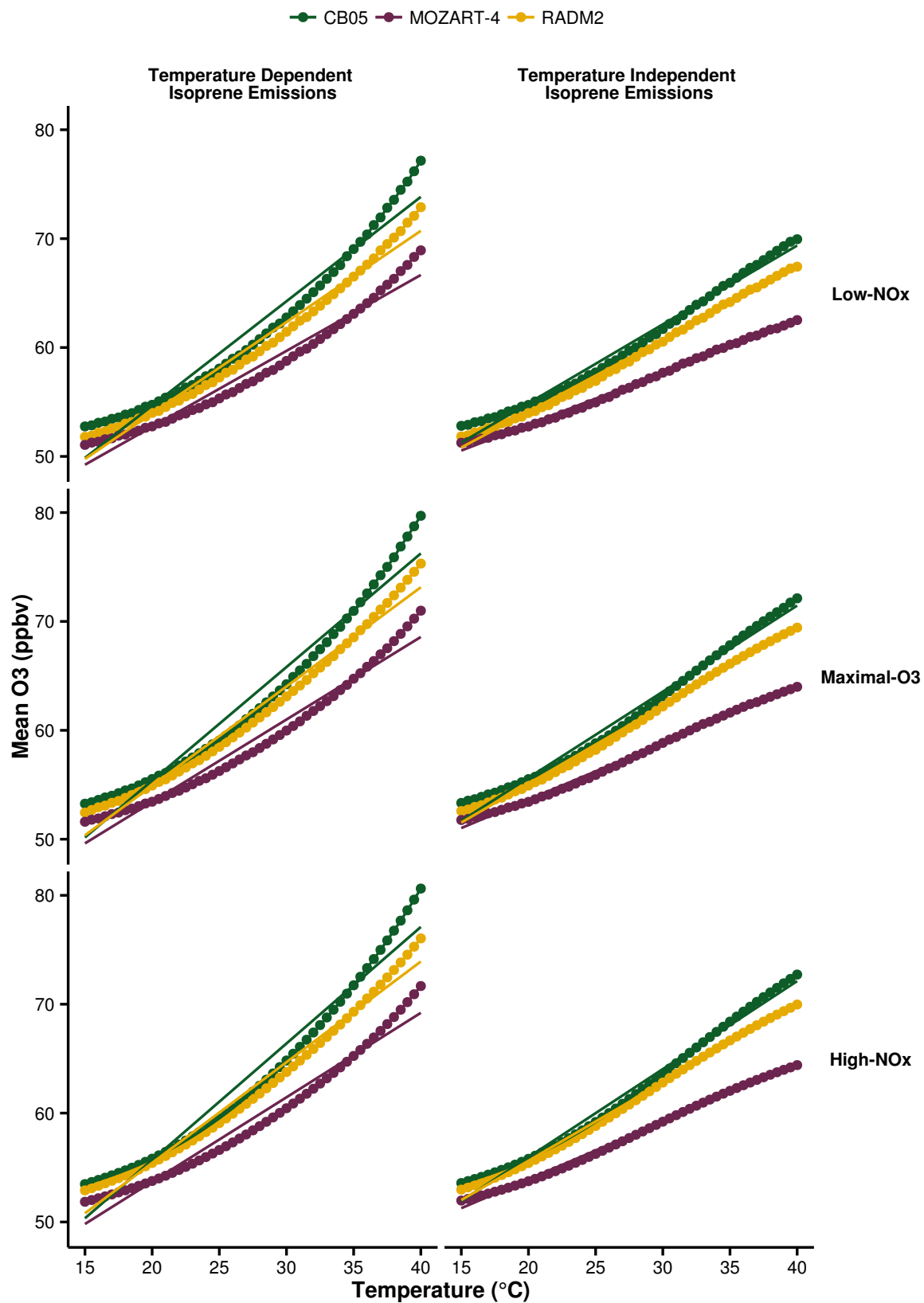
4 Discussion

5 Conclusions

References

- J. Coates and T. M. Butler. A comparison of chemical mechanisms using tagged ozone production potential (TOPP) analysis. *Atmospheric Chemistry and Physics*, 15(15):8795–8808, 2015.
- L. K. Emmons, S. Walters, P. G. Hess, J.-F. Lamarque, G. G. Pfister, D. Fillmore, C. Granier, A. Guenther, D. Kinnison, T. Laepple, J. Orlando, X. Tie, G. Tyndall, C. Wiedinmyer, S. L. Baughcum, and S. Kloster. Description and evaluation of the Model for Ozone and Related chemical Tracers, version 4 (MOZART-4). *Geoscientific Model Development*, 3(1):43–67, 2010.
- A. Guenther, T. Karl, P. Harley, C. Wiedinmyer, P. I. Palmer, and C. Geron. Estimates of global terrestrial isoprene emissions using MEGAN (Model of Emissions of Gases and Aerosols from Nature). *Atmospheric Chemistry and Physics*, 6(11):3181–3210, 2006.

Figure 3: Correlation of mean ozone mixing ratio with temperature in Low-NO_x, maximal-O₃ and High-NO_x conditions for each chemical mechanism. A linear relationship between mean ozone mixing ratios and temperature is inferred, regression statistics are found in Table 2.



162 A. B. Guenther, X. Jiang, C. L. Heald, T. Sakulyanontvittaya, T. Duhl, L. K. Emmons, and
 163 X. Wang. The Model of Emissions of Gases and Aerosols from Nature version 2.1 (MEGAN2.1):
 164 an extended and updated framework for modeling biogenic emissions. *Geoscientific Model*
 165 *Development*, 5(6):1471–1492, 2012.

166 M.E. Jenkin, L.A. Watson, S.R. Utembe, and D.E. Shallcross. A Common Representative
 167 Intermediates (CRI) mechanism for VOC degradation. Part 1: Gas phase mechanism development.
 168 *Atmospheric Environment*, 42(31):7185 – 7195, 2008.

169 J. J. P. Kuenen, A. J. H. Visschedijk, M. Jozwicka, and H. A. C. Denier van der Gon.
 170 TNO-MACC_II emission inventory; a multi-year (2003–2009) consistent high-resolution european
 171 emission inventory for air quality modelling. *Atmospheric Chemistry and Physics*, 14(20):
 172 10963–10976, 2014.

173 AsM Lourens. *Air quality in the Johannesburg-Pretoria megacity: its regional influence and*
 174 *identification of parameters that could mitigate pollution*. PhD thesis, North-West University,
 175 Potchefstroom Campus, 2012.

176 N. Passant. Speciation of UK emissions of non-methane volatile organic compounds. Technical
 177 report, DEFRA, Oxon, UK., 2002.

178 George Pouliot, Hugo A.C. Denier van der Gon, Jeroen Kuenen, Junhua Zhang, Michael D. Moran,
 179 and Paul A. Makar. Analysis of the emission inventories and model-ready emission datasets of
 180 Europe and North America for phase 2 of the AQMEII project. *Atmospheric Environment*, 115:
 181 345–360, 2015.

182 S. E. Pusede, D. R. Gentner, P. J. Wooldridge, E. C. Browne, A. W. Rollins, K.-E. Min, A. R.
 183 Russell, J. Thomas, L. Zhang, W. H. Brune, S. B. Henry, J. P. DiGangi, F. N. Keutsch, S. A.
 184 Harrold, J. A. Thornton, M. R. Beaver, J. M. St. Clair, P. O. Wennberg, J. Sanders, X. Ren,
 185 T. C. VandenBoer, M. Z. Markovic, A. Guha, R. Weber, A. H. Goldstein, and R. C. Cohen.
 186 On the temperature dependence of organic reactivity, nitrogen oxides, ozone production, and
 187 the impact of emission controls in San Joaquin Valley, California. *Atmospheric Chemistry and*
 188 *Physics*, 14(7):3373–3395, 2014.

189 Sally E. Pusede, Allison L. Steiner, and Ronald C. Cohen. Temperature and Recent Trends in
 190 the Chemistry of Continental Surface Ozone. *Chemical Reviews*, 115(10):3898–3918, 2015.

191 Andrew Rickard, Jenny Young, M. J. Pilling, M. E. Jenkin, Stephen Pascoe, and S. M. Saunders.
 192 The Master Chemical Mechanism Version MCM v3.2. <http://mcm.leeds.ac.uk/MCMv3.2/>,
 193 2015. [Online; accessed 25-March-2015].

194 D. Simpson, A. Benedictow, H. Berge, R. Bergström, L. D. Emberson, H. Fagerli, C. R. Flechard,
 195 G. D. Hayman, M. Gauss, J. E. Jonson, M. E. Jenkin, A. Nyíri, C. Richter, V. S. Semeena,
 196 S. Tsyro, J.-P. Tuovinen, Á. Valdebenito, and P. Wind. The EMEP MSC-W chemical transport
 197 model – technical description. *Atmospheric Chemistry and Physics*, 12(16):7825–7865, 2012.

198 William R. Stockwell, Paulette Middleton, Julius S. Chang, and Xiaoyan Tang. The second
 199 generation regional acid deposition model chemical mechanism for regional air quality modeling.
 200 *Journal of Geophysical Research: Atmospheres*, 95(D10):16343–16367, 1990.

201 E. von Schneidemesser, J. Coates, A. J. H. Visschedijk, H. A. C. Denier van der Gon, and T. M.
 202 Butler. Variation of the NMVOC speciation in the solvent sector and the sensitivity of modelled
 203 tropospheric ozone. *Atmospheric Environment*, page In preparation, 2015.

204 Greg Yarwood, Sunja Rao, Mark Yocke, and Gary Z. Whitten. Updates to the Carbon Bond
 205 Chemical Mechanism: CB05. Technical report, U. S Environmental Protection Agency, 2005.